



Study of the radionuclide deposition in the radioactive ion line of the Selective Production of Exotic Species (SPES) facility

A. Monetti ^a, A. Donzella ^{b,c,*}, M. Ballan ^a, L. Centofante ^a, S. Corradetti ^a, M. Ferrari ^d, G. Lilli ^{a,e}, M. Manzolaro ^a, T. Marchi ^a, D. Scarpa ^a, L. Zangrando ^f, A. Zenoni ^{b,c}, A. Andrichetto ^a

^a INFN, Laboratori Nazionali di Legnaro, Viale dell'Università 2, 35020 Legnaro (PD), Italy

^b Università degli Studi di Brescia, Dipartimento di Ingegneria Meccanica e Industriale, Via Branze 38, 25123 Brescia, Italy

^c INFN, Sezione di Pavia, Via A. Bassi 6, 27100 Pavia, Italy

^d Université Jean Monnet Saint-Etienne, CNRS, Institut d'Optique Graduate School, Laboratoire Hubert Curien UMR 5516, F-42023, Saint-Etienne, France

^e Università degli Studi di Padova, Dipartimento di Tecnica e Gestione dei sistemi industriali, Stradella S. Nicola 3, 36100 Vicenza, Italy

^f INFN, Sezione di Padova, Via F. Marzolo 8, 35131 Padova, Italy

ARTICLE INFO

Keywords:

SPES project
Radioactive ion beams
Monte Carlo

ABSTRACT

SPES (Selective Production of Exotic Species) is a second generation facility for the production of radioactive ion beams that is going to be commissioned at the Laboratori Nazionali di Legnaro of INFN at Legnaro, Padua, Italy. Radioactive neutron-rich isotopes are expected to be produced by nuclear fission induced by a 40 MeV, 200 μ A primary proton beam impinging on a ^{238}U target. The expected reaction rate is about 10^{13} fission/s. Radioactive ion beams are produced using the isotope separation on-line technique. The production of such an amount of radioactive species raises radiological issues throughout the life cycle of the facility. A study of the radioactive contamination of the components of the radioactive ion beam line is performed with the FLUKA Monte Carlo simulation code, under realistic hypotheses for the produced isobaric beams. The present results complete previous studies focused on the radiological impact of the production target irradiation, the residual activation of the primary proton beam line and the radioactive contamination of the ion source complex. The overall ambient dose equivalent rate due to the different radiation sources is calculated at several positions inside the production bunker and at different times after a typical one-year operating period of the facility with the ^{238}U target at full power. The obtained results and the developed methodology provide the guidelines and the needed tools to plan ordinary and extraordinary interventions as well as final decommissioning of the SPES facility.

1. Introduction

SPES (Selective Production of Exotic Species) is a second generation nuclear facility for the production of radioactive ion beams based on the ISOL (Isotope Separation On-Line) technique (Lindroos, 2004; Stora, 2013; Popescu et al., 2020). It is currently in advanced construction phase at INFN-LNL (Istituto Nazionale di Fisica Nucleare, Laboratori Nazionali di Legnaro), Padua, Italy (Gramegna et al., 2018).

The SPES production method is based on a primary proton beam of 40 MeV energy and 200 μ A current produced by a commercial cyclotron. Radioactive neutron-rich isotopes are produced by nuclear fission induced by the proton beam on a ^{238}U target at a rate of about 10^{13} fission/s. Thus, to produce the desired amount of a given single isotope, much higher amounts of different isotopes will be unavoidably produced in the ISOL target together with intense neutron fields.

In this context, safety is an essential aspect in the design of a high-intensity ISOL facility. The most relevant radiological issues to be taken into account are the following:

- the intense radiation levels produced by the facility during operations;
- the activation of the ^{238}U target due to fission products;
- the residual activity generated by: interactions of the primary proton beam; activation due to the intense neutron fields; deposition of radioactive ions inside the magnetic separators and other elements of the beam line;
- the volatile activity present in the target and in the ion source as well as in the related vacuum system.

As a consequence, the biological hazard connected with the production and handling of such radioactive ion species imposes severe

* Corresponding author at: Università degli Studi di Brescia, Dipartimento di Ingegneria Meccanica e Industriale, Via Branze 38, 25123 Brescia, Italy.
E-mail address: antonietta.donzella@unibs.it (A. Donzella).

radiological safety challenges to the design, operation, ordinary and extraordinary maintenance as well as final decommissioning of any ISOL facility.

As described later in Section 2, the so-called Front-End of the SPES facility consists of the portions of the Primary Proton Beam (PPB) line and of the Radioactive Ion Beam (RIB) line, with supporting structures, hosted inside a shielded production bunker. The unit containing the Target and the Ion Source (TIS) is located at the crossing of the two orthogonal PPB and RIB lines.

Previous studies were devoted to different radiological issues related to the irradiation of the SPES production targets and their whole life cycle (Andrighetto et al., 2005, 2006b; Monetti et al., 2015; Andrighetto et al., 2006a; Donzella et al., 2020b). During operation, the TIS unit suffers strong thermomechanical stresses due to the non-uniformity of the high power (8 kW) deposited by the primary beam on the target, as well as the degradation of the ion source material kept at 2000 °C by current heating. Therefore, the TIS unit must be regularly replaced with a fresh one. The high level of activation due to ^{238}U fission, larger than 10^{11} Bq, makes compulsory the use of automatic handling systems for its replacement. During routine operations, no operator access is allowed inside the production bunker in presence of an activated TIS unit.

More recently, the residual activation of the SPES Front-End, due to the primary proton beam and to the intense neutron fields produced by ^{238}U fission, has been studied by means of the two Monte Carlo codes MCNPX+CINDER'90 and FLUKA (Donzella et al., 2020a). Furthermore, the radioactive contamination of the ion source complex and, in particular, of its most critical component, the ion extraction electrode, has been studied (Centofante et al., 2021). The main aim of these studies was to predict the residual radiological hazard in different areas surrounding the SPES Front-End inside the production bunker, to define and implement strategies for the protection of the personnel involved in the operations of ordinary and extraordinary maintenance and final decommissioning. In these works, the level of residual activation of the SPES Front-End was assessed at different cooling times following the operation activities, throughout the facility life cycle.

The present study is an extension and a completion of the two previous works, and aims at evaluating the radioactive contamination of the components of the RIB line inside the production bunker, in particular of the electromagnetic elements used for mass separation and selection. The presented results, along with those from earlier studies, will enable the completion of the radiological map of the SPES production bunker at different times after a typical one-year operating period of the facility. With appropriate adjustments, the methodology developed in the present work can be extended to the case of other ISOL facilities.

The present paper is organized as follows. In Section 2, a short description of the SPES Front-End structure is given. Special emphasis is devoted to the RIB line and the components most likely affected by radioactive ion contamination during the SPES operations: the Wien filter, an electromagnetic device used as mass separator, and the downstream slits, used as mass selector. In Section 3, the Monte Carlo tools and the methods adopted for the calculation of the radioactive ion production and deposition on the RIB line are described.

In Section 4, the prediction of the ambient dose equivalent rate generated by the radioactive contamination of the RIB line in the production bunker at different cooling times is discussed. Realistic hypotheses for the most likely requested isobaric beams with the $^{238}\text{UC}_x$ target are adopted.

In Section 5, the overall ambient dose equivalent rate inside the production bunker is calculated, after a typical one-year operation of the facility with the $^{238}\text{UC}_x$ target at full power. The main contributions are the Front-End activation by the primary beam and neutron fields (Donzella et al., 2020a), the radioactive ion deposition in the ion source complex (Centofante et al., 2021) and the radionuclide deposition on the RIB line elements. In Section 6 conclusions are drawn.

2. The SPES project, an ISOL facility at LNL

SPES is an INFN project in advanced realization phase at LNL, Legnaro (Padua). Its main aim is the construction of a second generation ISOL facility for the production of post accelerated beams of neutron-rich radioactive nuclei (Prete et al., 2014; Andrighetto et al., 2018; Gramegna et al., 2018). The primary beam is constituted by 40 MeV protons provided by the 70p cyclotron from Best Cyclotron Systems (BCS, 2023) company, with a typical intensity of 200 μA at full power.

A high power $^{238}\text{UC}_x$ target (Monetti et al., 2015, 2016; Corradetti et al., 2021, 2017; Andrighetto et al., 2016) has been developed, in order to produce approximately 10^{13} fission/s on ^{238}U nuclei. The target is composed of seven disks, 40 mm diameter and 0.8 mm thickness, with a density of about 4 g/cm³.

The fission products are extracted by thermal processes, by keeping the target at high temperature (2000 °C) in high vacuum (10^{-6} mbar), and ionized to a 1+ charge state by an ion source. Three different ion sources can be used according to the requested beam: the Surface Ionization Source, the Plasma Ion Source and the Resonance Ionization Laser Ion Source (Manzolaro et al., 2017, 2014; Scarpa et al., 2012).

The Surface Ionization Source is realized in a tantalum hot cavity. It is very effective for low ionization potential elements such as alkali or alkaline-earth metals. The Resonance Ionization Laser Ion Source is structurally identical to a hot cavity ion source, but the atoms are irradiated with laser pulses, while kept in the gaseous phase in the cavity. The laser-induced ionization is highly selective for a wide range of elements, since a specific element can be ionized according to the chosen laser frequencies, although the atoms with low ionization potential remain as contaminants. In the Plasma Ion Source, electron impact ionization is used to ionize the atoms that are present in the gas phase inside the ion source. It is indicated for high ionization potential elements, but it is not very selective.

The produced ions are accelerated towards the ion extraction electrode by a potential difference up to 40 kV, mass separated and transported out of the production bunker. They are then sent to a second high-resolution mass separation and subsequently suffer a charge breeding before being re-accelerated in the ALPI superconducting LINAC at LNL. A previous SPES study discusses the radiation protection constraints related to the transport of the radioactive ion beams downstream of the production bunker (Sarchiapone and Zafiroopoulos, 2016).

The SPES facility will operate in cycles, one cycle being composed of 15 days of continuous irradiation followed by 15 days of beam off. This approach allows the short-lived radioisotopes produced in the target to decay to a large extent. Therefore, the residual activity of the TIS unit is reduced before it is removed by a dedicated remote handling vehicle (Lilli et al., 2023) to be transported to a shielded temporary storage (Donzella et al., 2020b). Typically, one year of facility operation is composed of ten operating cycles followed by a two-month stop for ordinary maintenance.

2.1. The SPES Front-End structure

In Fig. 1, the Front-End layout is shown. Along the PPB line (left part of the picture) different components are shown: (a) the graphite beam collimators and the collimator shielding structure; (b) the proton beam monitoring system; (c) the gate valve closing the PPB line needed to isolate it during the TIS unit extraction; (d) the proton bellow connecting the PPB to the TIS unit, and the PPB line supporting structure.

The TIS unit is located at the crossing of the PPB and RIB lines. It accounts for the following elements: (e) the target chamber body with the two gate valves, on the PPB line side and on the RIB line side, respectively; (f) the TIS unit supporting structure with its automatic sliding system; (g) the current supply circuit for target and ion source heating.

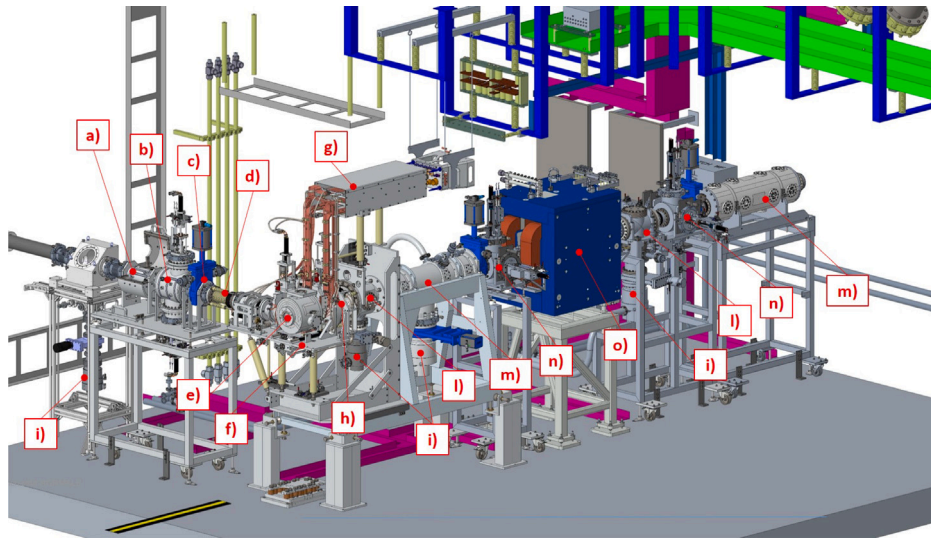


Fig. 1. The SPES Front-End layout. The PPB line is on the left side of the picture and the RIB line on the right side, orthogonal to the former one. The TIS unit is located at the crossing of the two beam lines. See text for a description of the components.

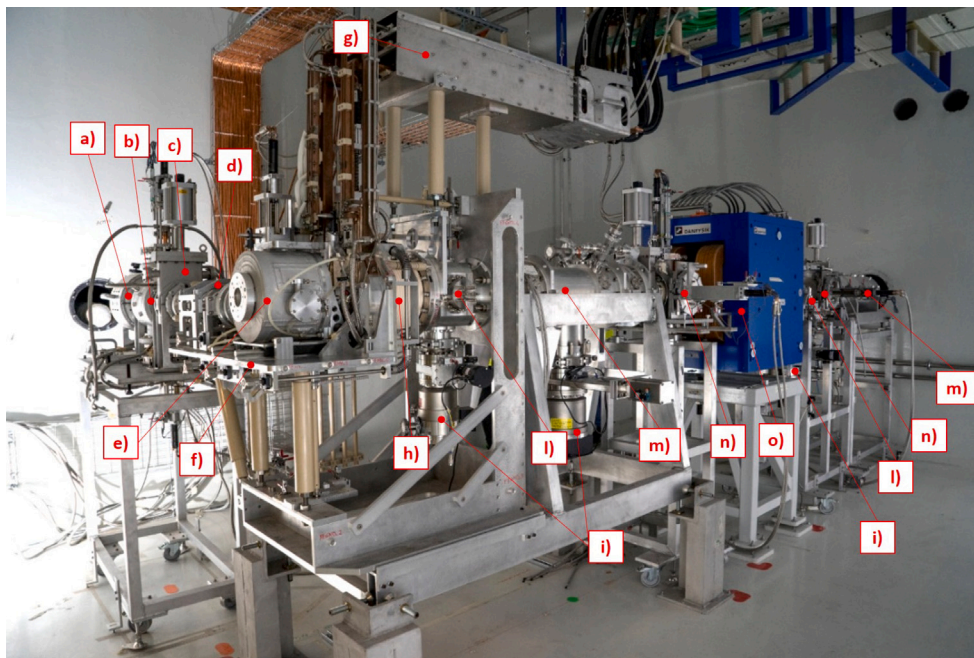


Fig. 2. Picture of the Front-End installed in the SPES production bunker at INFN-LNL. The description of the components is the same of Fig. 1.

On the RIB line side (right part of the picture) the following elements can be seen: (h) the first line segment containing the ion extraction electrode; (i) the turbo-molecular vacuum pumps; (l) the beam deflectors; (m) the triplets; (n) the diagnostic boxes, the first one equipped with a beam profiler and Faraday cup, and the second one similar to the first one, but with in addition the slits used for mass selection; (o) the Wien filter mass separator, with the copper coils highlighted in light brown.

Fig. 2 shows a picture of the Front-End installed inside the production bunker of the SPES building at INFN-LNL, ready for the commissioning.

Fig. 3 shows a cross section of the Wien filter structure and of the line elements downstream the Wien filter, where the deposition of the isotopes of the radioactive ion beam is studied. The main components are highlighted: (a) the Wien filter yoke; (b) the Wien filter electrodes;

(c) the mechanical coupling flange; (d) the beam deflectors; (e) the turbo-molecular pump; (f) the mass selection slits; (g) the second diagnostic box; (h) the second triplet.

3. Study of the radionuclide deposition along the RIB line

3.1. The simulation tools for geometry description and particle transport

FLUKA is a fully integrated Monte Carlo package for the simulation of transport and multiple physical processes of particles and nuclei interacting with matter (Ferrari et al., 2005; Böhlen et al., 2014). In FLUKA, the amount of unstable residual nuclei produced by inelastic hadronic interactions in all the modeled materials, their time evolution with generation of daughter nuclei, as well as the tracking of the

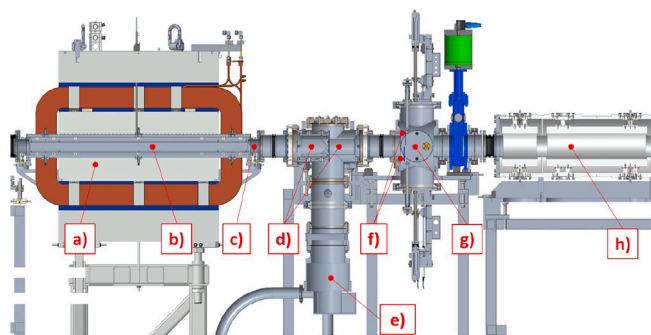


Fig. 3. Cross section of the Wien filter and downstream components of the RIB line. See text for the description of the components.

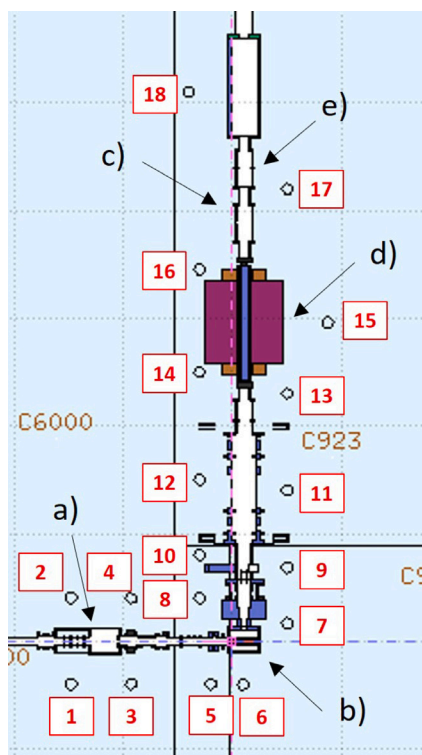


Fig. 4. Horizontal cross-section of the FLUKA Front-End geometry. Eighteen positions where the dose rate is evaluated are indicated by numbered circles. (a) PPB line; (b) TIS unit; (c) RIB line; (d) Wien filter; (e) mass selection slits.

emitted radiation, can be calculated according to a given irradiation history (Ferrari et al., 2005).

FLUKA was already used to simulate the primary proton beam inside the PPB line, accounting for the proton interactions with collimators and beam line elements, as well as the isotope production in the SPES target and fission neutron fields (Donzella et al., 2020a). It was also used to predict the isotope deposition on the extraction ion electrode tip and consequent contamination of the component (Centofante et al., 2021).

In the present paper, FLUKA is employed to model the geometry of the whole Front-End shown in Figs. 1–3, accounting for the different relevant components of the PPB line, of the TIS unit and, in particular, of the RIB line, including the Wien filter. In Fig. 4, the horizontal cross section of the FLUKA geometry at the nominal beam line height (150 cm), is shown.

Under realistic hypotheses for the produced isobaric beams, the radioactive ion deposition on the RIB line elements, the resulting residual

activation as well as the ambient dose equivalent rate $dH^*(10)/dt$ in the surroundings of the Front-End structure are predicted. The calculations are performed at different cooling times after several irradiation cycles of the target (see Section 4).

The dose rate sampling is performed at the eighteen selected points around the Front-End, highlighted with circles in Fig. 4. Each point is located 40 cm away from the Front-End structure and represents a position likely occupied by the personnel performing maintenance operations. The version used in the present study is FLUKA 2021.2.9 (INFN-FLUKA Team, 2023).

3.2. Radioactive contamination of the RIB line components

Downstream of the ion source and the ion extraction electrode, the radioactive line of the SPES Front-End includes several elements necessary to shape and transport the radioactive ion beam out of the production bunker. Most of them are electrostatic devices: the beam deflectors, able to correct the trajectory of the beam and align it to the beam axis center, and the quadrupole triplets that control the beam size and focus it through the beam pipe.

In addition, beam diagnostic devices are installed along the RIB line to monitor the beam current and profile. They are housed in vacuum chambers, closed by stainless steel flanges and are connected to special pneumatic motors, needed to provide their movement.

Vacuum required to transport the ion beam also prevents any spread of radioactive elements out of the beam lines. It is maintained by turbo molecular pumps located along the beam pipes. At the same time, the pumps evacuate the volatile radioisotopes from the Front-End beam pipes, channeling them to the gas recovery system (Buffa et al., 2021).

The Wien filter is a device that uses perpendicular electric and magnetic fields to select particles with a given velocity. It is able to perform a first mass separation of the mono-energetic ion beam coming from the extraction electrode with a mass resolution of around 1/100. The mass separation slits, located at the entrance of the second diagnostic box, are used as mechanical barrier to stop the unwanted slightly deflected beam.

The ions whose mass does not fall within the range selected by the Wien filter setting and by the aperture of mass separation slits are deposited on the radioactive beam line elements, both inside and downstream of the Wien filter. The radioactive isotopes spread mostly on the Wien filter electrodes, however, relevant amounts are deposited also on the beam deflectors after the Wien filter and on the mass selection slits.

The Wien filter contamination depends on the isotope beam required by the users and on the specific ion source employed to produce it. The continuous build-up of the radioactive isotopes sticking on the RIB line elements constitutes a radioactive source that becomes more and more critical with the accumulation of active periods of the SPES facility. This factor becomes especially significant when evaluating maintenance interventions close to the Wien filter.

A previous study on the radiation protection constraints related to the transport of the radioactive ions along the SPES RIB line, and in particular on the Wien filter, was performed using the FLUKA code for Monte Carlo simulation (Sarchiapone and Zafiroopoulos, 2016). As a result of this work, contributions to the ambient dose equivalent rate were assessed, considering both the activation of the materials of the Wien filter due to the intense neutron fields in the bunker, and the radionuclides stopped by the Wien filter during the extraction of the beam of interest.

The first contribution to the dose rate was calculated by FLUKA at 1 m distance from the Wien filter outer face, considering only one irradiation cycle, and resulted to be about 100 $\mu\text{Sv/h}$. The second contribution was evaluated after two years of extraction of a single specific radioactive isotope, ^{132}Sn , followed by some months of cooling time. Separate calculations for the build-up and decay of each stopped radionuclide were performed using simplified Bateman equations, then

the contribution from all sources were summed up to give the final result of about 3 mSv/h at 1 m distance from the Wien filter.

In the present study, a more comprehensive and general computation approach is developed. The FLUKA Monte Carlo code is employed to simultaneously evaluate the build-up and decay of all radioisotopes deflected by the Wien filter, assuming that different mass values, chosen on the basis of the main user requests, are selected.

Depending on the produced beam, the calculation of the different positions where the produced isotopes are deposited is performed, and the corresponding radioactive source sampled accordingly. The dose rate is then evaluated in the production bunker volume, especially in proximity of the devices located on the RIB line. Positions relevant for maintenance operations are reported in Fig. 4.

The calculation procedure is achieved in the following steps:

1. simulation of the isotope production in the target due to ^{238}U fission;
2. selection of the ionized isotopes forming the radioactive ion beam, accounting for the efficiency of the ionization process as well as the sticking properties of the volatile ions;
3. implementation of the FLUKA model, accounting for the calculated isotope deposition along the RIB line elements. The result of this step depends both on the mass value selected by the Wien filter and on the adopted ion source;
4. assumption for the production of isobaric beams in the first period of the SPES activity, in terms of selected masses and number of production cycles; molecular beams are not considered for the first years of activity of the facility;
5. calculation of the gamma ambient dose equivalent rate inside the Front-End bunker and its time evolution, based on an appropriate irradiation protocol for the first year of the SPES operations.

Step (1) was fulfilled in a previous work (Centofante et al., 2021). Steps (2) to (4) of this procedure are detailed in the following sections 3.2.1 and 3.2.2, whereas the results of step (5) are reported in Section 4.

3.2.1. Selection of radioactive isotopes forming the RIB

The ion deposition source implemented in FLUKA is composed of the portion of the 40 keV ion beam entering the ion extraction electrode that is not selected by the Wien filter and the mass selection slits and, therefore, deposits along the Wien filter and the downstream elements of the RIB line. In the present study, the Plasma Ion Source ionization method is assumed, since it is less selective and, therefore, the resulting RIB is richer in radioactive isotopes.

The radioactive isotopes used to build the FLUKA source of deposited ions are selected among the many isotopes produced in the target (Centofante et al., 2021), accounting for the decay chains of the radioactive isotopes, the efficiency of the adopted ionization method (Monetti et al., 2015), and following a set of appropriate selection criteria:

- the isotopes with production yields in the target lower than 10^8 nuclei/s are not accounted for, since previous studies allow us to consider that their relative contribution to the dose rate is negligible (Donzella et al., 2020b);
- the isotopes with mass greater than $M=200$ u are not considered, since they are isotopes of refractory elements and do not decay in non-refractory isotopes. Therefore they do not effuse out of the target;
- the isotopes of refractory elements (Y, Zr, Nb, Mo, Tc, Ru, Rh, La, Ce) that decay in non-refractory isotopes in less than 15 days are considered. 15 days is the time available for the radioactive elements to exit the target before the chamber is sealed at the end of the 15-day irradiation period; otherwise they do not leave the target at all;

- zero release time and unitary release efficiency for the effusing isotopes in the way from the target to the ion source are supposed (Monetti et al., 2015);
- for each isotope considered, the fission yield in the target is multiplied by the ionization efficiency value of the corresponding element in the ion source. These values were obtained by measurements performed at the ISOLDE Front-End Offline with the Plasma Ion Source. For noble gases, the obtained values are very close to other previous measurements (Alton, 1996). For elements like Cs, Ba, Rb, ionization efficiencies of the Surface Ionization Source are adopted, whereas, for the other elements, the adopted values are interpolated from the ones of neighboring elements. The final values of efficiencies range from 30% to 60% for the elements used for the deposition source;
- the volatile elements, such as Br, Kr, I and Xe for the SPES beam spectrum, deserve a particular mention. At the SPES extraction energies, above 20 keV, ions penetrate the materials (aluminum and stainless steel) and become trapped in the metal lattice up to a certain limit (Almén and Bruce, 1961; Brown and Davies, 1963; Carter et al., 1980; Oliver et al., 2001). This saturation value can be easily reached after a few days of stable beam operation. The following ions are scattered back and cannot be captured by the hit surfaces. In a conservative hypothesis, all the volatile isotopes with half-lives shorter than 1 year are considered, whereas the others are not considered in the calculations;
- concerning all the other isotopes, those that decay in stable or volatile isotopes in more than 1 hour and less than 1000 years are taken into account since, below the 1-hour threshold half-life, the relative contribution to the dose rate is less than a few percent.

The set of ionized isotopes selected with these criteria out of the isotopes produced in the ^{238}U target forms the RIB. It contains 341 isotopes, considering the metastable states separately from the relative ground states. With the facility working at full power, the total ion intensity amounts to $3.65 \cdot 10^{12}$ nuclei/s. The selected isotopes are shown in the nuclear landscape of Fig. 5, where the color scale expresses the isotope yield and the black squares are the stable elements.

3.2.2. Deposition of the deflected ions along the RIB line elements

The Wien filter acts as a velocity selector thanks to the simultaneous presence of an electric field E and a magnetic field B , both uniformly distributed in the space and perpendicular to each other and to the RIB line axis. The selected ion beam velocity is $v = E/B$. If the ion beam of a fixed energy is composed of ions having different masses, the ion velocity depends on its mass and the Wien Filter can be used as a mass separator.

For the purposes of the present work, and to keep our assumptions conservative, it is assumed that the Wien filter and the mass separating slits are able to extract only the isobars corresponding to the selected mass from the set of ions constituting the RIB. All the other radioactive ions are considered to be deflected away from the beam axis and are deposited on the RIB line elements.

The deposition points of the different ions along the RIB line mechanical structures are obtained by analytical calculation of the ion trajectories inside the Wien filter electrodes, and by geometrical tracking using FLUKA in the elements downstream of the Wien filter (Monetti, 2017; Donzella, 2021). The isobaric beams are supposed to have negligible size.

The corresponding FLUKA source accounts for both the deposition points of the different isobars along the RIB line and the yields of the isotopes reported in Fig. 5. It is implemented in the FLUKA geometry model of the Front-End.

The geometrical distribution of the deposited radioactive ions, with consequent build-up and decay times, depends on the mass value M selected by the Wien filter. Based on the foreseen scientific program of

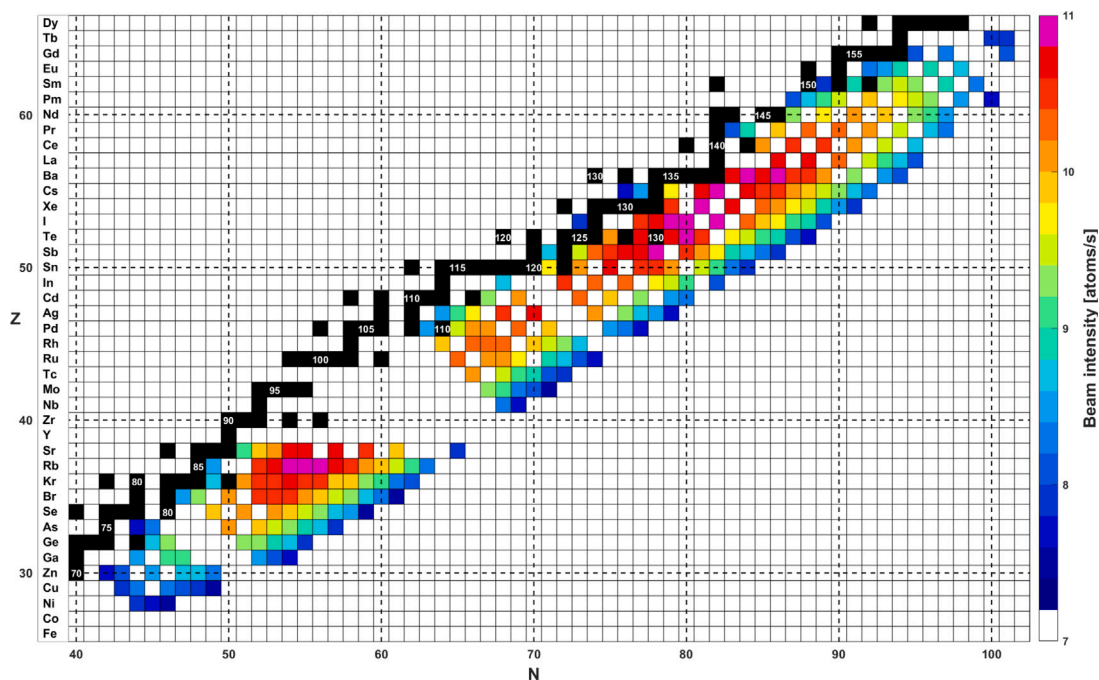


Fig. 5. Isotopes composing the radioactive ion beam with the Plasma Ion Source. With the facility working at full power, the total ion intensity amounts to $3.65 \cdot 10^{12}$ nuclei/s. The color scale represents the base-10 logarithm of the single isotope yield and the black squares are the stable elements.

the SPES facility (INFN Pisa, 2018; IUSS Istituto Universitario Studi Superiori, FERRARA, 2019), a realistic hypothesis for the isotope masses likely selected for the first period of the SPES activity with the $^{238}\text{U}_{\text{C}_x}$ target at full power is the following:

- mass $M = 95$ u, where ^{95}Rb and ^{95}Cs can be abundantly produced with the SPES Surface Ionization Source, and ^{95}Kr with the Plasma Ion Source;
- mass $M = 132$ u, where, in addition to the double magic ^{132}Sn , also ^{132}Te and ^{132}Sb can be produced with good rates.

4. External radiation exposure due to the RIB line contamination

The radioactive ions deflected by the Wien filter deposit on the Wien filter electrodes and on the elements of the RIB line such as the beam deflectors and the mass selection slits located before the second diagnostic box. Their deposition positions depend on the selected mass of the radioactive ion beam to be produced. Therefore, the dose rate calculated in the same points of the bunker as well as the temporal evolution of the dose rate is expected to be different for each isobaric beam produced.

As an illustrative example, the dose rate calculation is performed for the selected masses $M = 95$ u and $M = 132$ u, after 6 complete irradiation cycles at full power, that is after 15 days of cooling time following the end of the last shut down. This condition represents a critical scenario of access in the production bunker for extraordinary maintenance interventions, immediately after the removal of the irradiated TIS unit.

Fig. 6 and Fig. 7 show two horizontal meshes of the ambient dose equivalent rate $dH^*(10)/dt$, calculated for the masses $M = 95$ u and $M = 132$ u respectively. $H^*(10)$ represents an adequate assessment of the effective dose from photons in conditions of ISO rotational geometry, as in the case of the considered positions in the SPES production bunker.

Table 1 shows the values of $dH^*(10)/dt$ in some of the most critical positions around the RIB line, evidenced with red circles in Figs. 6 and 7. They refer to the masses $M = 95$ u and $M = 132$ u respectively, at different cooling times following 6 irradiation cycles: 15 days, 60 days, 6 months, 1 year, 2 years after the end of the last shut down. The

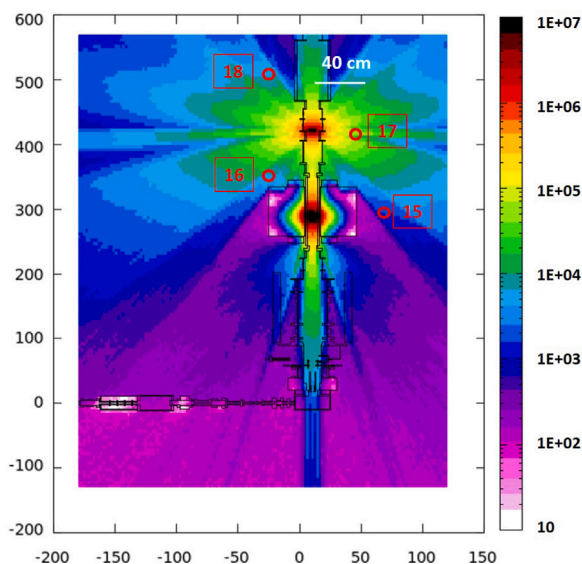


Fig. 6. Horizontal mesh of $dH^*(10)/dt$ in the SPES production bunker due to isotope deflection away from the RIB line, calculated for the mass $M = 95$ u passing the selection of the Wien filter. The mesh is calculated after 6 complete irradiation cycles. Red circles represent sampled positions on the mesh plane (150 cm height) as defined in Fig. 4. Units on the horizontal and vertical axes are in cm, units on the color scale are in $\mu\text{Sv/h}$.

conditions represented in Figs. 6 and 7 correspond to the dose rate values reported in the second column of Table 1.

In Fig. 8 and Fig. 9, the values of the ambient dose equivalent rate $dH^*(10)/dt$ as a function of time are shown for $M = 95$ u and $M = 132$ u respectively. They refer to the point 17, the closest to the mass selection slits, and are calculated after 1, 4, 6 and 10 irradiation cycles. The conditions represented in Figs. 8 and 9 for 6 irradiation cycles (gray line) correspond to the two rows relative to point 17 in Table 1.

The evolution of the dose rate as a function of the cooling time at point 17 is quite dependent on which mass is selected for delivery to

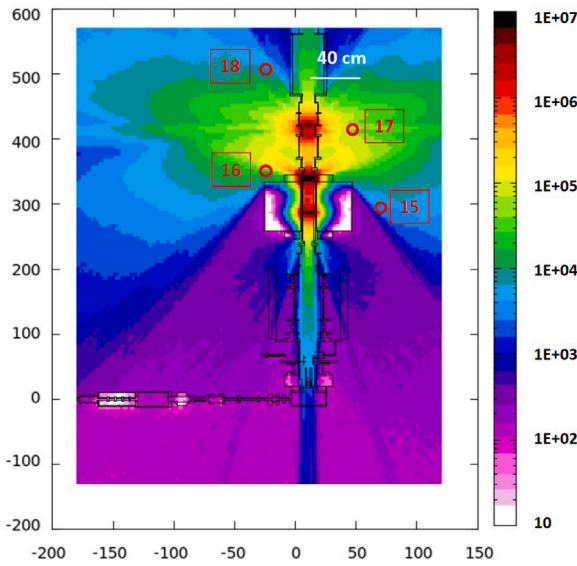


Fig. 7. The same as in Fig. 6, concerning the mass $M = 132$ u.

Table 1

Values of the ambient dose equivalent rate $dH^*(10)/dt$, due to the isotopes deflected by the Wien filter and deposited on the RIB line structures. They are calculated for the masses $M=95$ u and $M=132$ u, after 6 irradiation cycles, at different cooling times after the end of the last shut down (d =day, m =month, y =year). The values refer to the positions shown in red in Fig. 6 and Fig. 7. Units of $dH^*(10)/dt$ are $\mu\text{Sv/h}$. Monte Carlo errors are less than 1%.

$M=95$ u point N.	15 d	60 d	t_c 6 m	1 y	2 y
15	$2.8 \cdot 10^3$	$2.1 \cdot 10^3$	$7.0 \cdot 10^2$	$1.0 \cdot 10^2$	2.8
16	$4.8 \cdot 10^3$	$3.6 \cdot 10^3$	$1.2 \cdot 10^3$	$1.8 \cdot 10^2$	6.2
17	$5.4 \cdot 10^4$	$4.0 \cdot 10^4$	$1.4 \cdot 10^4$	$2.0 \cdot 10^3$	45
18	$6.0 \cdot 10^3$	$4.3 \cdot 10^3$	$1.5 \cdot 10^3$	$2.2 \cdot 10^2$	7.8

$M=132$ u point N.	15 d	60 d	t_c 6 m	1 y	2 y
15	$4.5 \cdot 10^3$	$3.8 \cdot 10^2$	69	58	48
16	$1.4 \cdot 10^4$	$1.3 \cdot 10^3$	$2.2 \cdot 10^2$	$1.8 \cdot 10^2$	$1.4 \cdot 10^2$
17	$6.8 \cdot 10^4$	$5.8 \cdot 10^3$	$1.3 \cdot 10^3$	$1.1 \cdot 10^3$	$8.8 \cdot 10^2$
18	$7.8 \cdot 10^3$	$7.1 \cdot 10^2$	$1.6 \cdot 10^2$	$1.2 \cdot 10^2$	97

experiments. Although the dose rate values are very similar 15 days after the end of the last shut down (apart from the first cycle), at longer times the behavior of the dose rate is very different. Up to 6 months the dose rate decreases much faster for $M = 132$ u; in fact, 6 months after the end of the last shut down, the dose rate for $M = 132$ u is a factor ten less than for $M = 95$ u. Conversely, from 6 months to 2 years, the dose rate falls much faster for $M = 95$ u than for $M = 132$ u. This depends on the very different isotope sets deposited on the beam line after the beam deflectors and on the slits.

With reference to the cross section of Fig. 3, the dose rate spatial distributions of Fig. 6 and Fig. 7 show that, for the mass $M = 95$ u, the isotopes are deposited mostly on the electrodes of the Wien filter and on the slits of the second diagnostic box. On the other hand, for the mass $M = 132$ u, they are also deposited on the coupling flange at the exit of the Wien filter and of the beam deflectors.

For the mass $M = 95$ u, the masses lower than $M = 89$ u and greater than $M = 101$ u stop inside the Wien filter. The same is true for the masses lower than $M = 124$ u and greater than $M = 141$ u, considering the mass $M = 132$ u. In both cases, the masses ranging between these limits are deposited on the structures between the exit of the Wien filter and the mass selection slits.

The most critical position for both masses is point 17, near the mass selection slits. As shown in Table 1, it accounts for a dose rate value

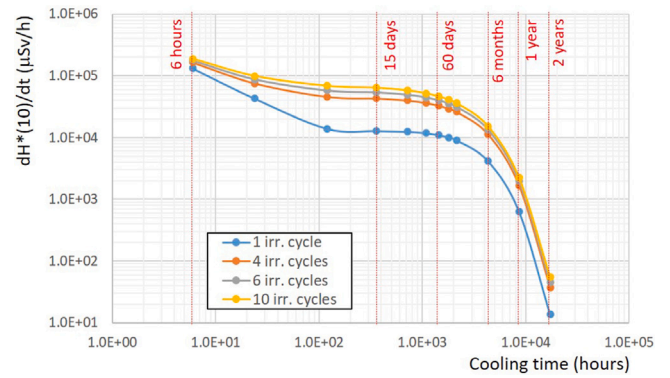


Fig. 8. Time evolution of the ambient dose equivalent rate $dH^*(10)/dt$ due to the isotope deflection from the RIB line, for the selected mass $M = 95$ u. The calculation is performed at point 17, for 1, 4, 6 and 10 irradiation cycles; it is sampled at different cooling times following the end of the last shut down, from 6 h until 2 years. The dose rate values are interpolated with a trendline.

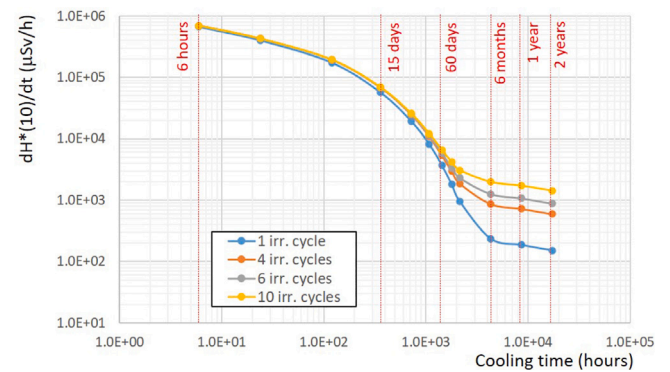


Fig. 9. The same as in Fig. 9, concerning the mass $M = 132$ u.

higher, even up to a factor of ten, than the values for the other points. In fact, the dose rate at point 17 exceeds 10 mSv/h for about 6 months of cooling, for $M = 95$ u, and for 45 days for $M = 132$ u, as shown in Figs. 8 and 9. Such high levels of dose rate also occur for the mass $M = 132$ u at point 16, near the exit flange of the Wien filter.

Instead, both meshes of Figs. 6 and 7 show that the Wien filter constitutes a good shield for gamma radiation, thanks to the high density of the iron and copper components. In fact, at point 15, the closest to the Wien filter, the dose rate level at all cooling times is up to 20 times lower when compared to that of point 17. A difference of a factor of ten is found also between point 17 and point 18, close to the second triplet, further away from the main structures of the RIB line where the ion deposition occurs.

The assessment of the ambient dose equivalent rate $dH^*(10)/dt$ in the areas close to the RIB line can help in optimizing the production sequence of the requested radioactive beams for different isotope masses, while minimizing the radiological hazard for maintenance interventions.

Indeed, in the hypothesis of producing the two aforementioned masses, the most convenient irradiation protocol for the first year of the SPES operations, with the $^{238}\text{UC}_x$ target at full power, could be the following: 6 consecutive irradiation cycles for the mass $M = 95$ u, followed by 4 consecutive irradiation cycles for the mass $M = 132$ u. The protocol foresees longer cooling times for the beam generating the larger dose rate at long times. This to minimize the residual dose rate when ordinary maintenance interventions occur, normally 2 months after the end of the last irradiation cycle.

Assuming this irradiation protocol, the contributions to the dose rate are calculated separately with FLUKA for each selected mass, and then

Table 2

Values of the ambient dose equivalent rate $dH^*(10)/dt$, due to the isotopes deflected by the Wien filter and deposited on the RIB line structures. They are calculated after 6 consecutive irradiation cycles for the mass $M=95$ u, followed by 4 consecutive irradiation cycles for the mass $M=132$ u. The sum of the two contributions is reported too. The cooling times considered for the two masses are 6 months for $M=95$ u and 2 months for $M=132$ u ($d=\text{day}$, $m=\text{month}$). Units of $dH^*(10)/dt$ are $\mu\text{Sv/h}$. Monte Carlo errors are less than 1%.

Point N.	$t_c=6$ m	$t_c=60$ d	Sum
	$M=95$ u	$M=132$ u	
15	$7.0 \cdot 10^2$	$3.6 \cdot 10^2$	$1.1 \cdot 10^3$
16	$1.2 \cdot 10^3$	$1.2 \cdot 10^3$	$2.4 \cdot 10^3$
17	$1.4 \cdot 10^4$	$5.3 \cdot 10^3$	$1.9 \cdot 10^4$
18	$1.5 \cdot 10^3$	$6.4 \cdot 10^2$	$2.1 \cdot 10^3$

summed to assess the total dose rate caused by all isotopes deposited on the RIB line in one year of activity. The results of these calculations are presented in Table 2 for the same positions of Table 1.

The obtained values of the total ambient dose equivalent rate $dH^*(10)/dt$, calculated for a period of one year of SPES activity with the $^{238}\text{UC}_x$ target at full power and reported in the last column of Table 2, are comparable, by order of magnitude, to the value of 3 mSv/h found in previous calculations (Sarchiapone and Zafiroopoulos, 2016) at 1 m distance from the Wien filter, after two years of ^{132}Sn beam extraction. This comparison can be made for point 17, taking in to account that it is located at 40 cm distance from the mass selection slits.

5. Global exposure due to the main radiation sources in the Front-End

5.1. Preliminary considerations

According to the ICRP recommendations (The International Commission on Radiological Protection, 2007), the assessment of the expected dose rate values for occupational exposure must provide indications to optimize operations or maintenance interventions on the Front-End all along its life cycle.

Different radiation “hot spots” have been identified inside the SPES production bunker. In addition to the radionuclide deposition in the RIB line elements, studied in Section 3, other radiation sources must be considered for the assessment of the total dose rate. The activation of the structures of the Front-End induced by interactions of primary proton beam and by fission neutrons (Donzella et al., 2020a), as well as the deposit of ions in the ion extraction electrode (Centofante et al., 2021), are particularly relevant.

In a planned exposure situation, as in the ordinary maintenance planned for the SPES facility, it can be assumed that each of these radiation sources contributes independently to the individual dose (The International Commission on Radiological Protection, 2007). Therefore, operators entering the production bunker for maintenance activities are exposed to a dose that is the sum of the components attributed to all these different radiation sources. These contributions are calculated separately.

The current dose limits at the LNL laboratories depend on the Italian regulations on the radiation protection (Repubblica Italiana, 2020), that limit the effective dose to a maximum of 1 mSv/year for public exposure and 20 mSv/year for occupational exposure. Moreover, the internal regulation of the LNL laboratories has adopted, as main radiation protection target on all SPES activities, the limitation of the effective dose to 0.5 mSv/year for public exposure and to 5 mSv/year for workers classified as exposed (Zafiroopoulos, 2010, 2018).

In general, a dose of a few hundred μSv per single ordinary intervention is judged reasonable, supposed that the intervention is necessary, infrequent and of limited duration. Otherwise, if maintenance interventions that incur higher doses are necessary, the subdivision of the exposure over several individuals can be considered with the purpose of optimizing the radiation protection.

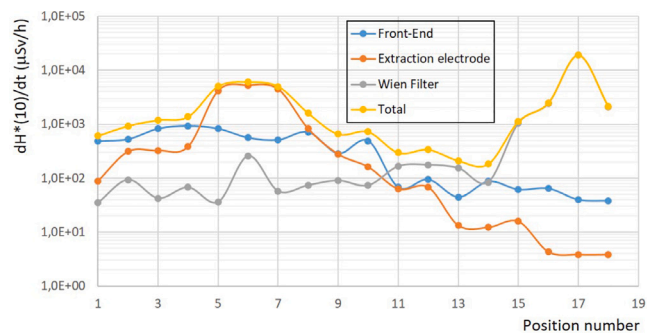


Fig. 10. Contributions to the ambient dose equivalent rate $dH^*(10)/dt$ from the Front-End residual activation (in blue), from the ion deposition on the extraction electrode (in orange) and on the RIB line (in gray), and their sum (in yellow). The values are calculated on all positions of Fig. 4, after 10 irradiation cycles and 60 day cooling time after the last shut down. The dose rate values are interpolated with a trendline.

5.2. Overall exposure assessment

In Fig. 10 the single contributions to the ambient dose equivalent rate $dH^*(10)/dt$ in the production bunker and their sum, calculated on all the positions of Fig. 4, are shown for the typical scenario of one year of SPES activity with $^{238}\text{UC}_x$ target at full power discussed in Section 4: 6 cycles with $M=95$ and 4 cycles with $M=132$, followed by 60 day cooling time after the last shut down.

The overall contribution to the ambient dose equivalent rate $dH^*(10)/dt$ after one year irradiation is in any position lower than 10 mSv/h, except for the positions downstream of the Wien filter. However, to optimize the worker protection during different maintenance operations, the reduction of the doses and of the dose rates to levels as low as reasonably achievable (ALARA) must be ensured.

The dose rates due to the Front-End residual activation (blue line) are generally lower than 1 mSv/h; the highest values correspond to the positions near the PPB line, due to proton activation of the graphite of the collimators, as well as in proximity of the TIS unit location and of the first part of the RIB line, due to neutron activation of the surrounding structures. In points 1–4, 8 and 10 this contribution is predominant.

Along the PPB line this specific problem was dealt with in the earliest design phases (Donzella et al., 2020a), with the implementation of a 10 mm lead shield surrounding the collimators and interposing graphite disks along the beam line to intercept scattered protons.

In points 5, 6 and 7, close to the TIS unit location and to the ion extraction electrode, the contribution to the dose rate due to the ion deposition on the ion extraction electrode (orange line) predominates. It is a factor ten higher than the one due to the Front-End residual activation, and a factor one hundred higher than the one due to the ion deposition on the Wien filter and the RIB line elements. For these positions, $dH^*(10)/dt$ values are a few mSv/h. The periodic replacement of the ion extraction electrode tip can contribute to reduce the dose rate up to a factor of 60% (Centofante et al., 2021).

The dose rate due to the isotopes deflected by the Wien filter and deposited along the RIB line (gray line) is generally not much above 100 $\mu\text{Sv/h}$. However, in points 16 and 18 located in proximity of the Wien filter and downstream, the dose rate values exceed 1 mSv/h and their contribution predominates. Furthermore, the last column of Table 2 shows that in point 17, near the mass selection slits of the diagnostic box, the dose rate is about 20 mSv/h.

Due to the high levels of gamma radiations, maintenance interventions close the Front-End, both ordinary and extraordinary, are in general considered as critical. The presence of lead shields near the beam collimators allows the surrounding dose rate levels to be limited to 1 mSv/h maximum. However, the dose rate levels are still high

enough to require a careful planning of the interventions along the PPB line.

The time required for the ordinary interventions close to the ion extraction electrode (point 7) must be carefully planned. After 10 irradiation cycles and 60 day long cooling time, a permanence of 10 min close to the ion extraction electrode corresponds to about 800 μSv of dose for the operator, a value considered too high for a single intervention. For this reason, the replacement of the ion extraction electrode before carrying out any other interventions in the surrounding area is strongly suggested. The possibility of a manual or semi-automatic handling for the extraction electrode has already been studied in detail (Centofante et al., 2021).

Finally, caution must be adopted in planning maintenance operations in the final section of the RIB line, downstream of the Wien filter, in particular in zones close to the second diagnostic box. However, these zones are far from the ^{238}U target, which constitutes an intense neutron radiation source, and are also shielded by the Wien filter dense structure. Therefore, radiation damage of the components is less likely and the need of maintenance interventions should be much less probable. In case of need of extraordinary intervention in this area, thanks to the available space surrounding this section of the RIB line, mobile shields for the protection of the operators can be easily adopted.

As a concluding remark, it is worth emphasizing that, in a conservative approach, the assumptions made so far lead, in general, to an overestimation of the calculated dose rates.

Concerning the contribution from the ion deposition on the extraction electrode, the ionization efficiency of the ion source was set to zero (Centofante et al., 2021); this means that all neutral atoms can reach the ion extraction electrode tip and stick upon it.

The deposition source constituted by the ions deflected by the Wien filter and deposited along the RIB line is built considering an ionization efficiency evaluated with the Plasma Ion Source, that is the least selective. Moreover, unitary release efficiency is set, and all the refractory isotopes that transmute in non-refractory isotopes in less than 15 days are considered, as if they are generated in the target at the beginning of the irradiation period. Finally, volatile isotopes that decay into non-volatile atoms with half-lives shorter than one year are considered, assuming that they remain trapped inside the material.

6. Conclusions

In the present study, a methodology is developed for the calculation of the radioactive contamination of the components of the RIB line of the SPES facility after one year of activity with the ^{238}U target at full power.

The FLUKA Monte Carlo simulation code is used for the calculation of the isotope production in the target due to ^{238}U fission, the ion deposition downstream of the mass separator device, the Wien filter, and the prediction of gamma ambient dose equivalent rate around the Front-End and its time evolution. The radioactive isotopes forming the ion deposition are extracted from the many isotopes produced in the target, accounting for the relative decay chains, the efficiency of the ionization method, and following a set of appropriate selection criteria.

The obtained results are analyzed together with the results of previous studies devoted to determine the residual activation of the SPES Front-End, due to the primary proton beam, and the radioactive contamination of the ion source complex, at different times during and after the target irradiation. Thus, the complete map of the overall radiation hazard inside the SPES production bunker can be calculated.

The results correspond to a typical one-year period of SPES activity at full power. However, the developed methodology can be applied to any possible use of the facility, including any combination of extracted isobaric radioactive ion beams as well as any intervention condition considered, ordinary and extraordinary maintenance, and final decommissioning. It can also be adapted to the operational conditions of other ISOL facilities.

After one year activity and 60 days cooling time following the last shut down, the values of the ambient dose equivalent rate $dH^*(10)/dt$ are a few mSv/h close to the TIS unit location and the ion extraction electrode, and larger than 10 mSv/h near the mass selection slits downstream the Wien filter. In other positions close to the Front-End, the calculated values are of the order of 1 mSv/h or less. In particular, thanks to the high density of the iron and copper components of the Wien filter, this device, where a large part of the separated radioactive ion beam is deposited, constitutes a good shield for gamma radiation.

In conclusion, any foreseen ordinary and extraordinary maintenance interventions on the SPES Front-End appear achievable with quite standard procedures, apart from the final part of the RIB line, where the radioactive ion deposition on the mass selection slits determines high levels of ambient dose equivalent rate in all studied conditions. For maintenance operations in this area, specific mitigation interventions and protection procedures should be defined by the authorities.

CRedit authorship contribution statement

A. Monetti: Writing – original draft, Visualization, Validation, Software, Methodology, Investigation, Formal analysis, Data curation, Conceptualization. **A. Donzella:** Writing – review & editing, Writing – original draft, Visualization, Validation, Software, Methodology, Investigation, Formal analysis, Data curation, Conceptualization. **M. Ballan:** Software, Conceptualization. **L. Centofante:** Validation, Software, Data curation, Conceptualization. **S. Corradetti:** Investigation, Conceptualization. **M. Ferrari:** Writing – review & editing, Software, Methodology, Conceptualization. **G. Lilli:** Writing – review & editing, Methodology, Investigation, Conceptualization. **M. Manzolaro:** Investigation, Conceptualization. **T. Marchi:** Validation, Conceptualization. **D. Scarpa:** Investigation, Conceptualization. **L. Zangrando:** Software, Data curation. **A. Zenoni:** Writing – review & editing, Writing – original draft, Validation, Supervision, Project administration, Methodology, Investigation, Formal analysis, Conceptualization. **A. Andrighetto:** Supervision, Project administration, Investigation, Formal analysis, Conceptualization.

Declaration of competing interest

The authors declare that they have no known competing financial interests or personal relationships that could have appeared to influence the work reported in this paper.

Data availability

Data will be made available on request.

Acknowledgments

The results published in the present paper were achieved using CloudVeneto, the Cloud infrastructure obtained from the integration between the “Cloud Area Padovana” (INFN) and the Cloud of ten departments of the University of Padua (Andretto et al., 2019).

References

- Almén, O., Bruce, G., 1961. Collection and sputtering experiments with noble gas ions. *Nucl. Instrum. Methods* 11, 257–278. [http://dx.doi.org/10.1016/0029-554x\(61\)90026-x](http://dx.doi.org/10.1016/0029-554x(61)90026-x).
- Alton, G., 1996. Targets and ion sources for RIB generation at the Holifield Radioactive Ion Beam Facility. *Nucl. Instrum. Methods Phys. Res. A* 382 (1–2), 207–224. [http://dx.doi.org/10.1016/s0168-9002\(96\)00632-8](http://dx.doi.org/10.1016/s0168-9002(96)00632-8).
- Andretto, P., et al., 2019. Merging OpenStack-based private clouds: the case of CloudVeneto.it. In: Forti, A., Betev, L., Litmaath, M., Smirnova, O., Hristov, P. (Eds.), *EPJ Web Conf* 214, 07010. <http://dx.doi.org/10.1051/epjconf/201921407010>.
- Andrighetto, A., Antonucci, C., Cevolani, S., Petrovich, C., 2006a. ENEA contribution to the design of the thin target for the SPES project. In: *ENEA FIN-P815-020* (2006). pp. 1–40.

- Andrighetto, A., Antonucci, C.M., Cevolani, S., Petrovich, C., Leitner, M.S., 2006b. Multifoil UCx target for the SPES project –An update. *Eur. Phys. J. A* 30 (3), 591–601. <http://dx.doi.org/10.1140/epja/i2006-10144-3>.
- Andrighetto, A., Cevolani, S., Petrovich, C., 2005. Fission fragment production from uranium carbide disc targets. *Eur. Phys. J. A* 25 (1), 41–47. <http://dx.doi.org/10.1140/epja/i2005-10064-8>.
- Andrighetto, A., et al., 2016. The SPES High Power ISOL production target. *Il Nuovo Cimento* 38 C 194, 1–4. <http://dx.doi.org/10.1393/ncc/i2015-15194-x>.
- Andrighetto, A., et al., 2018. SPES: An intense source of Neutron-Rich Radioactive Beams at Legnaro. *J. Phys. Conf. Ser.* 966, 012028. <http://dx.doi.org/10.1088/1742-6596/966/1/012028>.
- BCS, 2023. URL <http://www.bestcyclotron.com>. Accessed November 2023.
- Böhlen, T.T., Cerutti, F., Chin, M.P.W., Fassò, A., Ferrari, A., Ortega, P.G., Mairani, A., Sala, P.R., Smirnov, G., Vlachoudis, V., 2014. The FLUKA code: Developments and challenges for high energy and medical applications. *Nucl. Data Sheets* 120, 211–214. <http://dx.doi.org/10.1016/j.nds.2014.07.049>.
- Brown, F., Davies, J.A., 1963. The effect of energy and integrated flux on the retention and range of inert gas ions injected at keV energies in metals. *Can. J. Phys.* 41 (6), 844–857. <http://dx.doi.org/10.1139/p63-092>.
- Buffa, P., Giardina, M., Prete, G., De Ruvo, L., 2021. Fuzzy FMECA analysis of radioactive gas recovery system in the SPES experimental facility. *Nucl. Eng. Technol.* 53 (5), 1464–1478. <http://dx.doi.org/10.1016/j.net.2020.11.011>.
- Carter, G., Armour, D.G., Donnelly, S.E., Ingram, D.C., Webb, R.P., 1980. The injection of inert gas ions into solids: Their trapping and escape. *Radiat. Eff.* 53 (3–4), 143–173. <http://dx.doi.org/10.1080/00337578008207113>.
- Centofante, L., et al., 2021. Study of the radioactive contamination of the ion source complex in the Selective Production of Exotic Species (SPES) facility. *Rev. Sci. Instrum.* 92 (5), 053304. <http://dx.doi.org/10.1063/5.0045063>.
- Corradetti, S., et al., 2017. Graphene derived lanthanum carbide targets for the SPES ISOL facility. *Ceram. Int.* 43 (14), 10824–10831. <http://dx.doi.org/10.1016/j.ceramint.2017.05.106>.
- Corradetti, S., et al., 2021. The SPES target production and characterization. *Nucl. Instrum. Methods Phys. Res. B* 488, 12–22. <http://dx.doi.org/10.1016/j.nimb.2020.12.003>.
- Donzella, A., 2021. Risk Assessment of Radiation "Hot Spots" in a Radioactive Ion Beam Facility (Ph.D. Thesis). Department of Mechanical and Industrial Engineering, Brescia University, Italy.
- Donzella, A., et al., 2020a. Residual activation of the SPES Front-End system: a comparative study between the MCNPX and FLUKA codes. *Eur. Phys. J. A* 56 (2), <http://dx.doi.org/10.1140/epja/s10050-020-00068-1>.
- Donzella, A., et al., 2020b. Shielding analysis of the SPES targets handling system and storage area using the Monte Carlo code FLUKA. *Nucl. Instrum. Methods Phys. Res. B* 463, 169–172. <http://dx.doi.org/10.1016/j.nimb.2019.05.069>.
- Ferrari, A., Sala, P., Fassò, A., Ranft, J., 2005. FLUKA: A Multi-Particle Transport Code. Technical Report, Office of Scientific and Technical Information (OSTI), <http://dx.doi.org/10.2172/877507>.
- Gramegna, F., et al., 2018. The SPES exotic beam ISOL facility: Status of the project, technical challenges, instrumentation, scientific program. *Il Nuovo Cimento* 41 C 195, 1–7. <http://dx.doi.org/10.1393/ncc/i2018-18195-3>.
- INFN-FLUKA Team, 2023. INFN FLUKA. URL <http://www.fluka.org>. Accessed November 2023.
- INFN Pisa, 2018. SPES one-day Workshop: Probing fundamental symmetries and interactions by low energy excitations with SPES RIBs. URL <https://agenda.infn.it/event/13891>. Accessed November 2023.
- IUSS Istituto Universitario Studi Superiori, FERRARA, 2019. Interdisciplinary aspects and applications related to the SPES project. URL <https://agenda.infn.it/event/16937>. Accessed November 2023.
- Lilli, G., et al., 2023. Remote handling of radioactive targets at the SPES facility. *Il Nuovo Cimento* 46 C 32, <http://dx.doi.org/10.1393/ncc/i2023-23032-y>.
- Lindroos, M., 2004. Review of ISOL-type radioactive beam facilities. In: *Proceedings of EPAC 2004*, Lucerne, Switzerland (2004). pp. 45–49.
- Manzolaro, M., Andrighetto, A., Meneghetti, G., Monetti, A., Scarpa, D., Rossignoli, M., Vasquez, J., Corradetti, S., Calderolla, M., Prete, G., 2014. Ongoing characterization of the forced electron beam induced arc discharge ion source for the selective production of exotic species facility. *Rev. Sci. Instrum.* 85 (2), 02B918. <http://dx.doi.org/10.1063/1.4857175>.
- Manzolaro, M., D'Agostini, F., Monetti, A., Andrighetto, A., 2017. The SPES surface ionization source. *Rev. Sci. Instrum.* 88 (9), 093302. <http://dx.doi.org/10.1063/1.4998246>.
- Monetti, A., 2017. Design and Development of the Target-Ion Source System for the SPES Project (Ph.D. Thesis). Department of Industrial Engineering, Padua University, Italy, URL <https://hdl.handle.net/11577/3426200>. Accessed November 2023.
- Monetti, A., et al., 2015. The RIB production target for the SPES project. *Eur. Phys. J. A* 51 (10), 128. <http://dx.doi.org/10.1140/epja/i2015-15128-6>.
- Monetti, A., et al., 2016. On-line test using multi-foil SiC target at iThemba LABS. *Eur. Phys. J. A* 52 (6), 168. <http://dx.doi.org/10.1140/epja/i2016-16168-0>.
- Oliver, B.M., Eiden, G.C., Ballou, N.E., 2001. Implantation and Release of Krypton with Copper Foils. PNNL-13642, Pacific Northwest National Laboratory.
- Popescu, L., Hougbo, D., Dierckx, M., 2020. High-power target development for the next-generation ISOL facilities. *Nucl. Instrum. Methods Phys. Res. B* 463, 262–268. <http://dx.doi.org/10.1016/j.nimb.2019.05.023>.
- Prete, G., et al., 2014. The SPES project at the INFN- Laboratori Nazionali di Legnaro. *EPJ Web Conf* 66, 11030. <http://dx.doi.org/10.1051/epjconf/20146611030>.
- Repubblica Italiana, 2020. Decreto Legislativo 31 luglio 2020 n. 101, Attuazione della Direttiva 2013/59/Euratom, and subsequent additions and amendments Decreto Legislativo 25/11/2022 n. 203.
- Sarchiapone, L., Zafiropoulos, D., 2016. Radiation protection considerations along a radioactive ion beam transport line. *Int. J. Mod. Phys. Conf. Ser.* 44, 1660238. <http://dx.doi.org/10.1142/s2010194516602386>.
- Scarpa, D., Vasquez, J., Tomaselli, A., Grassi, D., Biasetto, L., Cavazza, A., Corradetti, S., Manzolaro, M., Montano, J., Andrighetto, A., Prete, G., 2012. Studies for aluminum photoionization in hot cavity for the selective production of exotic species project. *Rev. Sci. Instrum.* 83 (2), 02B317. <http://dx.doi.org/10.1063/1.3673628>.
- Stora, T., 2013. Recent developments of target and ion sources to produce ISOL beams. *Nucl. Instrum. Methods Phys. Res. B* 317, 402–410. <http://dx.doi.org/10.1016/j.nimb.2013.07.024>.
- The International Commission on Radiological Protection, 2007. The 2007 recommendations of the international commission on radiological protection. *Ann. ICRP* 37 (2-4), ICRP Publication 103.
- Zafiropoulos, D., 2010. Relazione tecnica in materia di radioprotezione relativa al progetto SPES - Fase alfa dei Laboratori Nazionali di Legnaro dell'INFN.
- Zafiropoulos, D., 2018. Relazione Tecnica dell'Esperto Qualificato in Materia di Radioprotezione Relativa al progetto SPES - Fase Beta - dei Laboratori Nazionali di Legnaro dell'INFN.